

Considerations on minimum friction velocity

By E. AKYLAS¹, Y. TSAKOS¹, M. TOMBROU^{1†} and D. P. LALAS²

¹*Laboratory of Environmental Physics, University of Athens, Greece*

²*National Observatory of Athens, Greece*

(Received 8 May 2001; revised 6 January 2003)

SUMMARY

The concept of the minimum friction velocity is studied using three different methods of scalar averaging for the calculation of the stresses. Particular emphasis is given to the extraction of the influence of a non-zero ambient wind shear observed in field measurements. Data from three different experimental sites in Athens with high roughness values are analysed in order to provide information concerning the dependence of the dimensionless minimum friction velocity on the dimensionless roughness length. Data from the BOREX-95 experiment have also been re-analysed according to the methodologies presented in this study. The results are compared to the large-eddy simulations that are considered to be a reference study on shear-free convection.

KEYWORDS: Ambient wind shear Convection Large-eddy simulations Vector and scalar averaging

1. INTRODUCTION

During the last decade, it has been recognized that convective boundary layers (CBLs) are affected by large eddies. These eddies produce essential convergence/divergence flow patterns in the surface layer, even in the absence of a mean wind (Businger *et al.* 1971; Businger 1973; Schumann 1988; Sykes *et al.* 1993; Beljaars 1995; Zilitinkevich *et al.* 1998), resulting in turbulence production. Thus, even in zero mean wind a minimum friction velocity W_* could be determined.

The velocity scale inherent in such cases is the Deardorff (1970, 1972) convective velocity-scale:

$$W_* = (B_{\text{sfc}}h)^{1/3}. \quad (1)$$

Here, h is the CBL height and B_{sfc} the buoyancy flux at the surface, which is related to the surface potential temperature flux, Q_{sfc} , by:

$$B_{\text{sfc}} = \frac{g}{\theta} Q_{\text{sfc}}, \quad (2)$$

where g is the acceleration due to gravity, and θ is the potential temperature. The surface-layer scaling could be extended to include the Deardorff velocity scale, W_* , and consequently h .

The extension of the traditional Monin–Obukhov (M–O) theory to include the shear-free convection case, takes shape through the concept of the scalar wind speed, V_s , defined as:

$$V_s^2 = \mathbf{V}^2 + V_{\text{gust}}^2 \quad (3)$$

where \mathbf{V} is the vector wind speed and V_{gust} is the gustiness wind speed due to the convective eddies. In the case of zero mean vector wind, the scalar wind speed equals V_{gust} .

The gustiness wind speed has been suggested to be proportional to W_* by numerous theoretical schemes (see Schumann 1988; Sykes *et al.* 1993; Beljaars 1995; Zilitinkevich *et al.* 1998):

$$V_{\text{gust}} = \beta W_* \quad (4)$$

† Corresponding author: Environmental Physics Laboratory, University of Athens, Panepistimioupolis, GR-15784 Zografou, Greece. e-mail: mtombrou@cc.uoa.gr

where β is a dimensionless coefficient. Strictly speaking, β depends on the reference height z , since the gustiness wind fits a profile $\beta(z)W_*$ for a non-slip condition at the surface. A constant value of β assumes that the reference level lies outside the inner layer attached to the convective eddies, i.e. $\beta = \text{constant}$ corresponds to $z \rightarrow \infty$. However, taking into account that the shape of the profile becomes rapidly uniform, the dependence of β is weak for the standard level of $z = 10$ m (Grachev *et al.* 1998).

In shear-free convection the traditional friction velocity, u_* , which in this case vanishes, should be replaced by the minimum friction velocity, U_* (Businger 1973). Correspondingly, the traditional M–O length, L , is replaced by the relevant convective surface-layer length, L_* :

$$L_* = \frac{U_*^3}{k B_{\text{sfc}}} = \frac{U_*^3 h}{k W_*^3}, \quad (5)$$

where k is the Von Karman constant.

Businger (1973) proposed that the dimensionless minimum friction velocity U_*/W_* is a universal unknown function of the dimensionless roughness length z_0/h . According to all previous researchers, this function can theoretically be approached if a wind profile is applied to V_{gust} , through an equation of the form:

$$\frac{U_*}{W_*} = \beta k \left\{ \ln \left(\frac{h_{\text{sfc}}}{z_0} \right) - \Psi_u \left(\frac{h_{\text{sfc}}}{L_*} \right) + \Psi_u \left(\frac{z_0}{L_*} \right) \right\}^{-1}, \quad (6)$$

where Ψ_u are empirical similarity functions. Differences between the various theoretical schemes concern the definition of the surface-layer height, h_{sfc} , where β approaches a constant value, as well as the shape of the profiles through the determination of Ψ_u . Their empirical coefficients, wherever these exist, were estimated by fitting to available data. Schumann (1988), Sykes *et al.* (1993) and Beljaars (1995) used data from large-eddy simulations (LESs; Schmidt and Schumann 1989; Sykes *et al.* 1993). Zilitinkevich *et al.* (1998) utilized data from field measurements from the Tropical Ocean–Global Atmosphere Coupled Ocean–Atmosphere Response Experiment (TOGA COARE; Fairall *et al.* 1996), the San Clemente Ocean Probing Experiment (SCOPE; Kropfli and Clifford 1994) and BOREX-95 (Mikkelsen *et al.* 1996).

In this study, the calculation of the dimensionless minimum friction velocity U_*/W_* under strong instability is examined using data from three different experimental sites in the greater Athens area. These experiments were conducted at sites with high values of roughness, z_0 , thus new information is added to the previous work presented in Akylas *et al.* 2001. Particular emphasis is given to the methodology appropriate for extracting a possible influence of a non-zero wind shear. Data from the BOREX-95 experiment have been re-analysed using the methodologies discussed here.

2. THEORETICAL CONSIDERATIONS

(a) Reconsidering minimum friction velocity

Akylas *et al.* 2001 showed that, despite the physical differences among the theoretical schemes (Eq. (6)), the coefficient β plays the key role in their results for the minimum friction velocity. Higher values of β (> 1.5) are found for the experimental data, while the LESs are satisfied by values of β close to unity. This systematic difference between field and LES data could be simply explained by the contribution of the mean wind shear to the near-surface mixing. Indeed, the LESs simulated genuine shear-free convection which is practically never observed in nature. In the real world, field data are always affected by some shear.

During such ‘pseudo shear-free’ convective conditions, the contribution of the mean vector wind speed could be included in a parameter C , so that:

$$V_s = C\beta W_*. \quad (7)$$

C is derived by combining Eqs. (3), (4) and (7), so that:

$$C = \sqrt{1 + \frac{\mathbf{V}^2}{\beta^2 W_*^2}} = \sqrt{1 + \frac{\mathbf{V}^2}{V_s^2 - \mathbf{V}^2}}. \quad (8)$$

Since, according to Businger (1973), U^*/W^* is a universal function of z_0/h , parameter β could be a universal constant and is physically well specified. On the other hand, C is a quantitative expression of the influence of the vector wind on the value of the scalar wind. Up to now, the fitting of the theoretical schemes to experimental data has considered the combined influence of C and β exclusively in terms of β . This is due to the fact that all data were assumed to be representative of shear-free convection. However, a background flow and a non-zero vector wind were present. This accounts for the larger values of β given by the theoretical schemes for field data, in contrast to their fitting to LES data where, due to the vanished wind speed, $C = 1$.

Following this concept, it is reasonable to conclude that field data have up to now measured a dimensionless friction velocity u_*/W_* , larger than the minimum one (U_*/W_*). Therefore, in order to fit Eq. (6) to field data, it should be modified as:

$$\frac{u_*}{W_*} = C\beta k \left\{ \ln \left(\frac{h_{\text{sfc}}}{z_0} \right) - \Psi_u \left(\frac{h_{\text{sfc}}}{L} \right) + \Psi_u \left(\frac{z_0}{L} \right) \right\}^{-1}. \quad (9)$$

Both Eqs. (6) and (9) refer to a constant value of β , thus they both apply for the specific height h_{sfc} , which is the top of the surface layer. However, they both can be extended in order to be applicable for any measurement height within the surface layer. This is done by substituting the constant value of β by an unknown function of $\beta(z)$ that actually corresponds to the dimensionless gustiness wind profile $V_{\text{gust}}(z)/W_*$. Under this concept, a combination of Eqs. (6) and (9) can be derived, resulting in

$$\frac{U_*}{W_*} = \frac{1}{C} \frac{u_*}{W_*} \frac{\left\{ \ln \left(\frac{z}{z_0} \right) - \Psi_u \left(\frac{z}{L} \right) + \Psi_u \left(\frac{z_0}{L} \right) \right\}}{\left\{ \ln \left(\frac{z}{z_0} \right) - \Psi_u \left(\frac{z}{L_*} \right) + \Psi_u \left(\frac{z_0}{L_*} \right) \right\}}, \quad (10)$$

which is a possible way to extract the mean flow contribution from field data so as to return to the minimum friction velocity, U_*/W_* . In Eq. (10), u_*/W_* , as well as parameters C , z_0 , h and L are derived directly from experimental data, while L_* is implicitly related to U_*/W_* through Eq. (5). The elimination of $\beta(z)$, which can be considered a universal constant only at the top of the surface layer, provides the possibility of applying this equation at any level inside the surface layer. It should also be noted that the roughness lengths, z_0 , appearing in the numerator and denominator of Eq. (10) are not necessarily equal. This is more important in the case of surfaces with moveable roughness elements (sea, sand, etc.). A similar remark could be considered for the stability functions, Ψ_u , if more appropriate formulations are provided for the shear-free convection case. The most important issue regarding Eq. (10) is the calculation of u_* from experimental data, since the traditional vector averaging of the stresses becomes inadequate under very low wind speeds. In such a case, the use of the scalar average concept needs to be considered in more detail.

Unlike vector averaging, scalar averages return zero only in the case of motionless air. This holds true for wind speed, as well as for stress averages. Although scalar wind speed is well documented (Mahrt *et al.* 1996; Grachev *et al.* 1998; Zilitinkevich *et al.* 1998), less work has been done concerning scalar averaged stresses. Grachev *et al.* 1998 and Zilitinkevich *et al.* 1998, proposed a scalar averaging for the calculation of stresses, but such a method has never been applied to field data up to now. In this study a first attempt is made, in order to distinguish and investigate vector and scalar averaged stresses.

(b) *Calculation of flow properties by vector and scalar averaging*

The principal idea followed here is based on the averaging procedure described in Mahrt *et al.* (1996). According to this, the turbulent fluctuations of a quantity are decomposed into two parts: a non-organized part that refers to small-scale turbulence; and a semi-organized part which can be linked with long-period flows in the atmosphere such as large eddies, sea-breezes etc. This decomposition can be realized by considering two different time-scales: the local averaging length, t , which isolates the non-organized part, and the total averaging length, T , which is larger than t to increase the sample size. The special case of $t = T$ is obviously the common way to decompose a quantity into its mean value and deviation.

Scalar averaging (r.m.s. of the local averages) can be applied to the wind speed through the following equation:

$$V_{s\{t,T\}} = \sqrt{\langle \langle \mathbf{V} \rangle_t^2 \rangle_T}, \quad (11)$$

where the notation $\langle A \rangle_B$ refers to the mean value of quantity A averaged within the time-scale B . This equation is equivalent to decomposing scalar wind speed as

$$V_{s\{t,T\}}^2 = \mathbf{V}^2 + \sigma^2 \langle u_x \rangle_t + \sigma^2 \langle u_y \rangle_t, \quad (12)$$

where u_x and u_y are the components of the horizontal wind vector, and \mathbf{V} refers to the T -averaged vector wind speed. The quantity $\sigma^2 \langle u_x \rangle_t + \sigma^2 \langle u_y \rangle_t$ is the variance of the semi-organized part of the flow in the total averaging scale. Comparing to Eq. (3), this sum can play the role of the gustiness wind speed added to the vector wind.

If the averaging procedure of the two time-scales (t , T) is considered, the vector-averaged stresses are given by:

$$\begin{aligned} \langle u'_x u'_z \rangle_{\{t,T\}} &= \langle u_x u_z \rangle_T - \langle u_x \rangle_T \langle u_z \rangle_T - \langle \langle u_x \rangle'_t \langle u_z \rangle'_t \rangle_T, \\ \langle u'_y u'_z \rangle_{\{t,T\}} &= \langle u_y u_z \rangle_T - \langle u_y \rangle_T \langle u_z \rangle_T - \langle \langle u_y \rangle'_t \langle u_z \rangle'_t \rangle_T, \end{aligned} \quad (13)$$

where $\langle u_x \rangle'_t$, $\langle u_y \rangle'_t$ and $\langle u_z \rangle'_t$ are the deviations of the local average $\langle u_x \rangle_t$, $\langle u_y \rangle_t$ and $\langle u_z \rangle_t$ from the total average $\langle u_x \rangle_T$, $\langle u_y \rangle_T$ and $\langle u_z \rangle_T$, respectively. The first two terms on the right-hand side (r.h.s.) of the previous equations correspond to the traditional (use of only one time-scale) averaging of stresses, expressed as $\langle u'_x u'_z \rangle_{\{T,T\}}$ and $\langle u'_y u'_z \rangle_{\{T,T\}}$ following the notation used here. Thus, Eqs. (13) can be rewritten as:

$$\begin{aligned} \langle u'_x u'_z \rangle_{\{t,T\}} &= \langle u'_x u'_z \rangle_{\{T,T\}} - \langle \langle u_x \rangle'_t \langle u_z \rangle'_t \rangle_T, \\ \langle u'_y u'_z \rangle_{\{t,T\}} &= \langle u'_y u'_z \rangle_{\{T,T\}} - \langle \langle u_y \rangle'_t \langle u_z \rangle'_t \rangle_T. \end{aligned} \quad (14)$$

Consequently, using these expressions, the vector averaged friction velocity is given as:

$$u_{*\{t,T\}} = (\langle u'_x u'_z \rangle_{\{t,T\}}^2 + \langle u'_y u'_z \rangle_{\{t,T\}}^2)^{1/4}. \quad (15)$$

The disadvantage of this formulation for u_* is that it results in zero for zero mean wind, since the stresses given by Eq. (14) are eliminated for sufficiently long averaging times.

It is, therefore, an apparent requirement to consider scalar averaging of the stresses in order to avoid the obvious weakness of Eq. (15) in cases of shear-free convection. The scalar averaged friction velocity is hereafter noted as \tilde{u}_* , in contrast to the vector averaged u_* in Eq. (15). Since there is no generally accepted formulation for the scalar stresses, several approaches are examined.

Following the scalar averaging procedure presented for the wind speed (Eq. (11)), \tilde{u}_* can be considered to be the scalar average of the t -scaled friction velocities, u_{*t} :

$$\tilde{u}_{*(a)}^2 = \langle u_{*t}^2 \rangle_T = \langle (\langle u'_x u'_z \rangle_t^2 + \langle u'_y u'_z \rangle_t^2)^{1/2} \rangle_T. \quad (16)$$

This friction velocity is the r.m.s. of the u_{*t} and is similar to what Schmidt and Schumann (1989), calculated as the minimum friction velocity from their LESs. Similarly, if scalar averaging is directly applied to the t -scaled stresses as proposed by Zilitinkevich *et al.* (1998), then \tilde{u}_* is given by:

$$\tilde{u}_{*(b)}^4 = \langle (\langle u'_x u'_z \rangle_t^2 + \langle u'_y u'_z \rangle_t^2) \rangle_T = \langle u_{*t}^4 \rangle_T, \quad (17)$$

which actually corresponds to the r.m.s. of the t -scaled stresses. In addition to the above, the suggestion of an anonymous referee was also considered as an option, giving \tilde{u}_* as:

$$\tilde{u}_{*(c)} = \langle (\langle u'_x u'_z \rangle_t^2 + \langle u'_y u'_z \rangle_t^2)^{1/4} \rangle_T = \langle u_{*t} \rangle_T. \quad (18)$$

This approach resembles the method used by Sykes *et al.* (1993) in order to derive the minimum friction velocity from their LES data. However, unlike Eqs. (16) and (17), which are connected to the scalar wind determination of Eq. (11), this formulation seems to be equivalent to a scalar wind of the following form:

$$V_{s\{t,T\}} = \langle |\mathbf{V}|_t \rangle_T. \quad (19)$$

From Eqs. (16), (17) and (18) it follows that: $\tilde{u}_{*(b)} > \tilde{u}_{*(a)} > \tilde{u}_{*(c)}$.

(c) Extracting the ambient wind shear

The use of scalar averaging offers the advantage of a non-zero result in the case of a vanished mean wind, so the above formulations are more appropriate than vector stresses for the calculation of friction velocity in convective near shear-free conditions. In order to make the minimum friction velocity coherent in such conditions (discussed in section 2(a)), experimental data should be handled in such a way as to eliminate the influence of vector wind. This can be performed by the use of Eqs. (16), (17) and (18) on real data, along with a procedure for the extraction of the ambient wind contribution from their results. Such a procedure, as discussed previously, is the application of Eq. (10) to the friction velocities defined by Eqs. (16), (17) and (18). However, based on an attractive mathematical similarity rather than on the physical sequence for the determination of the semi-organized part of the scalar wind in Eq. (12), the following expression for the minimum friction velocity can be suggested:

$$\tilde{U}_{*(a)}^2 = \tilde{u}_{*(a)}^2 - u_{* \{t,T\}}^2. \quad (20)$$

This corresponds to the standard deviation of the friction velocity. In the same sense, the standard deviation of the stresses would correspond to a minimum friction velocity given as:

$$\tilde{U}_{*(b)}^4 = \tilde{u}_{*(b)}^4 - u_{* \{t,T\}}^4. \quad (21)$$

Equation (12) defines the gustiness wind speed as the standard deviation of the locally averaged speed. In the case of Eq. (12) the resulting speed is physically sound, since it corresponds to a part of the kinetic energy which could be available for extra mixing or enhancement of fluxes in general. On the other hand, unlike energy (and consequently speed) the stresses and the forces are much more dependant on their vector character. Regarding the r.m.s. value of u_{*t} that Schmidt and Schuman (1989) used for calculating the minimum friction velocity from their LESs, it coincides with the standard deviation of u_{*t} (Eq. (20)), since in the LES the vector average of u_{*t} equals zero. As a result, Eq. (20) corresponds exactly to those LES results.

A similar relation could not be considered for $\tilde{u}_{*(c)}$, since it is linked to a scalar wind (Eq. (19)), different from the one considered in this study (Eq. (11)). In this averaging scheme, which is similar to the Sykes *et al.* (1993) LES method, the extraction can only be done as it has been stated in section 2(a). In this way Eq. (18) is used to calculate the friction velocity, u_* , appearing in Eq. (10). Since $\tilde{u}_{*(c)}$ yields the smallest value among Eqs. (16)–(18), it is apparent that the relevant minimum friction velocities obtained through Eq. (10) will follow the same order. It should also be mentioned that the application of Eq. (10) is subject to the additional uncertainty of defining the appropriate stability correcting function, in contrast to Eqs. (20) and (21) which are only affected by experimental uncertainties.

3. APPLICATION TO EXPERIMENTAL DATA

Calculation of the minimum friction velocity, using all previously suggested methods, is performed by analysis of experimental data from three different sites. The selection of cases approaching shear-free convection is done according to specific criteria and the appropriate averaging time-scale is defined by spectral analysis. Furthermore, in order to present the dimensionless friction velocity versus the dimensionless length z_0/h , the mixing height corresponding to the time of each selected case and the roughness length at each site are estimated.

(a) *Measurement sites*

Three datasets from different sites in the greater Attiki peninsula area are used; these are presented in Fig. 1. The National Observatory of Athens (hereafter NOA) is located near the Athens city centre and Marousi (hereafter MAR) is a suburban area in the northern outskirts of the city. Datasets for MAR and NOA were acquired during an earlier experimental campaign carried out during August and September 1994 (Batcharova and Gryning 1998). Measurements of the three velocity components u , v and w , and the virtual temperature T_v were taken by Kaijo-Denki DAT/TR-61B sonic anemometers with a sampling frequency of 10 Hz at a height of 15 m AGL. The semi-rural suburban site of Pikermi (hereafter PIK) is located far from the built area of Athens at the foot of Penteli mountain. The measurement campaign at PIK was conducted from 15 February to 8 June 1999 by NOA in the framework of the EU SFINCS Project (Larsen and Zilitinkevich 2001). Measurements of u , v , w and T_v were taken using a CSAT3 (Campbell Scientific) Sonic Anemometer Thermometer with a sampling frequency of 8 Hz at 18.8 m AGL. A limited number of radiosonde measurements were also made at PIK from 28 May to 7 June 1999, during various time periods. Additionally, the 00 and 12 UTC radiosondes from the Elliniko Airport of Athens (hereafter LGAT) were provided by the Hellenic National Meteorological Service for the whole period of both experimental campaigns. Finally, the historical dataset of the BOREX-95 experiment



Figure 1. Map of the Attiki peninsula. The three mountains surrounding the central Athens area, Immitos (1024 m AMSL), Penteli (1140 m AMSL) and Parnitha (1450 m AMSL) are marked, as well as the locations of the Pikermi (A), Marousi (B) and National Observatory of Athens (C) sites (PIK, MAR and NOA, respectively, in the text). The Elliniko airport of Athens is marked as (D). The elevation contours are plotted at 100 m intervals. The shoreline is depicted by a thick line.

(Mikkelsen *et al.* 1996) was available for recalculation in order to apply the concepts discussed in this study.

(b) Estimation of mixing height

Among the three sites in Attiki, a direct estimation of the mixing height at PIK could only be made from the radiosonde data available during the last 10 days of the campaign. These measurements indicate a variety of temperature inversions between 500 and 1500 m in daytime hours.

Since no radiosonde data were available at NOA and MAR, as well as PIK, for the first 3 months of the campaign, the mixing height information has been sought from the 12 UTC LGAT radiosondes. A comparison of the available PIK radiosondes with the relevant LGAT data, led to the conclusion that for southerly flows the atmospheric structure at high altitudes is similar for both sites. This justifies the use of LGAT radiosondes as representative of the upper-air conditions for all three sites in the case of southerly winds. Therefore, combining a site's surface temperature with the relevant temperature profile, the typical mixing height values for each site at 12 UTC were estimated; these correspond to approximately 1400 m for PIK, 800 m for MAR and 1200 m for NOA.

In order to evaluate the diurnal variation of the mixing height, another approach was implemented, namely applying a theoretical estimate of the mixing height through integration of the surface heat flux obtained from sonic measurements (Stull 1988). When this method is applied to all three sites it allows a quantitative view of the

time evolution of the mixing height. Thus, combining this technique with the above arguments, it was possible to assign a specific value of the mixing height in every case.

(c) *Data analysis*

The three datasets were analysed in order to select cases as close as possible to the free-convection regime. The obvious choices are clear cloudless days and low wind speeds; in particular, days with normal distribution of heat flux were selected, as well as time intervals with wind speeds less than 3 m s^{-1} . Data from just after sunrise and before sunset were excluded in order to avoid transition periods. Variations of wind direction were studied thoroughly in order to exclude cases where the flow changed direction, e.g. during sea-breeze development. Since measurements of turbulence under light winds are affected by sampling errors, particular attention was given in the selected datasets to the vector averaged stresses within the local time-scale, $\langle u'w' \rangle_t$, that were found to be opposite to the respective mean wind vector, $\langle U \rangle_t$, in at least 90% of the t -averaged time intervals. Apart from the use of z/L to define instability, the approach to shear-free conditions can also be quantified by the calculation of parameter C (Eq. (8)). It is apparent that in free convection $C = 1$. In this study only cases with $1 < C < 2.25$ were selected, which correspond to a ratio of gustiness to vector wind speed of at least $1/2$.

According to the theoretical considerations of section 2(b), a primary goal is the definition of the time averaging-scales. The total averaging length, T , is chosen to be equal to 1 h; so all cases selected refer to this scale. The definition of the local averaging-scale, t , was determined by analysing the selected time-series of wind speed by FFT (fast Fourier transform). The resulting spectra, which are assumed to approximate shear-free convection, were compared to the analytical formulation for convective spectra of Højstrup (1982), and the fitting was indeed satisfactory for all cases selected from all three sites. The maximum of the theoretical curve obtained from the fitting represents the prevailing eddy-scale in each case. Each maximum defines a particular value for t , which is assigned to the respective case. These values range from 10 to 30 minutes. The averaging procedure is performed using each particular t and $T = 1 \text{ h}$.

In the case of the recalculation of flow properties from the BOREX-95 data, such a procedure was not possible due to the unavailability of the whole data series. Therefore, a characteristic length $t = 10 \text{ minutes}$ was assigned to all cases. The total averaging-scale was also 1 h in this case. For the BOREX-95 dataset all other parameters involved, that is mixing height and roughness length, were assigned values as in Zilitinkevich *et al.* (1998).

(d) *Estimation of roughness length*

The roughness length, z_0 , can be calculated from turbulence measurements by the use of the neutral drag coefficient, C_{Dn} , which is given by:

$$C_{Dn}^{-1/2} = \frac{1}{k} \ln \left(\frac{z}{z_0} \right) = \frac{V}{u_*} + \frac{1}{k} \left\{ \Psi_u \left(\frac{z}{L} \right) - \Psi_u \left(\frac{z_0}{L} \right) \right\}. \quad (22)$$

The stability correction function, Ψ_u , used in this analysis, is interpolated between the Kansas-type formulation (Paulson 1970) and a convective one (Fairall *et al.* 1996), as described in Grachev *et al.* (2000). Such a formulation gives a good agreement with the standard Kansas-type expressions for near-neutral stratification, and obeys the $-1/3$ asymptotic convective limit. The wind speed, V , and the friction velocity, u_* , are calculated from the experimental datasets, using the vector and scalar averaging

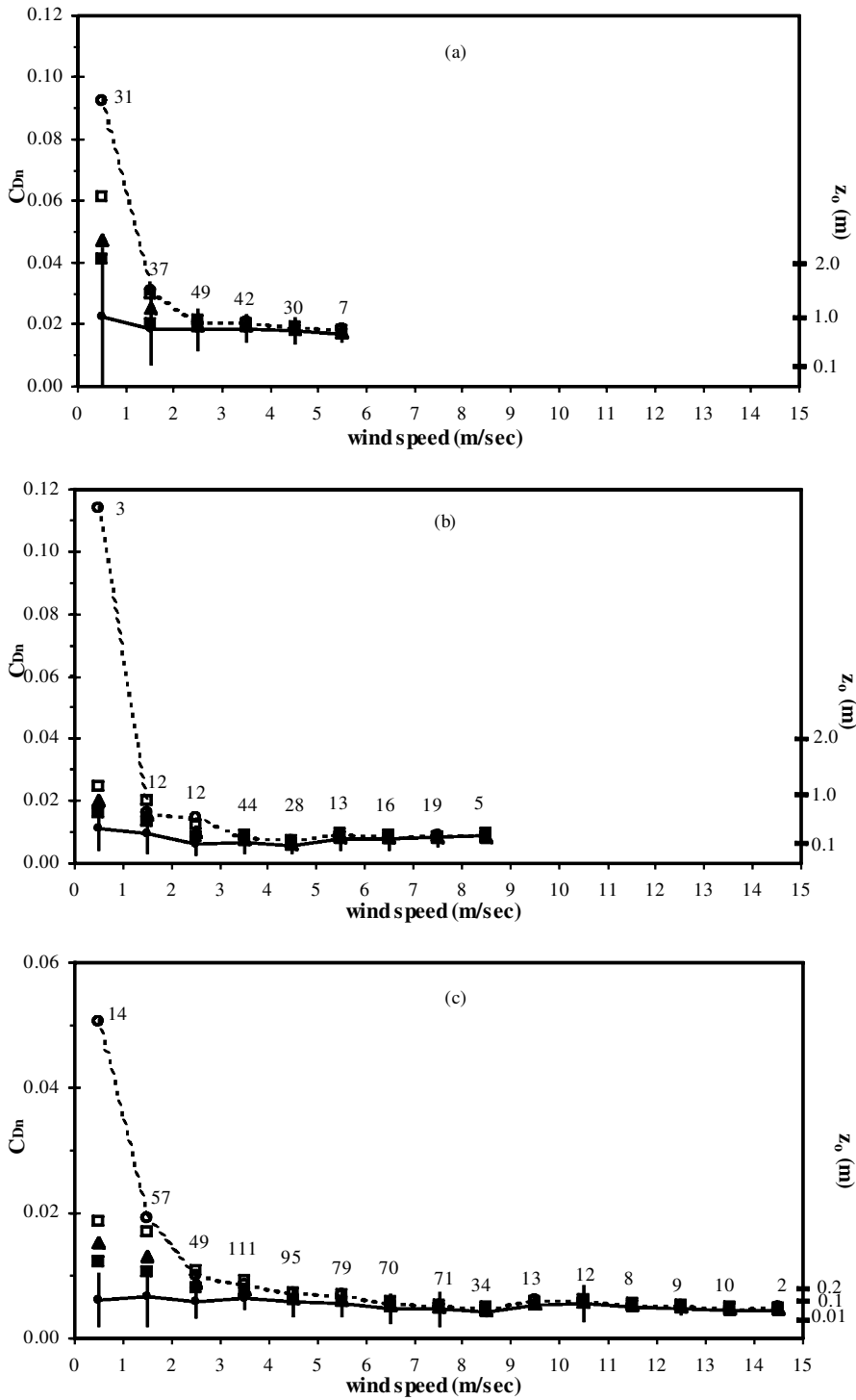


Figure 2. Neutral drag coefficient, C_{Dn} , values against roughness length, z_0 , for: (a) MAR, (b) NOA, and (c) PIK (see Fig. 1), calculated using vector wind and stress (Eq. (15); \circ), scalar wind (Eq. (11)) and vector stress (Eq. (15); \bullet) and scalar stresses by Eq. (16) (\blacktriangle), Eq. (17) (\square) and Eq. (18) (\blacksquare).

procedures described in section 2(b) The results of these calculations for all wind speed intervals are presented in Fig. 2. Furthermore, the following discussion demonstrates the differences amongst the various averaging techniques.

The traditional C_{Dn} values correspond to the vector-averaged wind speed, V_v , and stresses, u_* (Eq. (15)). This averaging leads to extremely large values at low wind speeds (Fig. 2). The use of the scalar wind, V_s , instead (Eq. (11)), seems to be appropriate for vector-averaged stresses in all wind speed classes. In other words, it results in a desirably constant value, which coincides with the traditional calculation at high wind speeds (neutral case). When scalar-averaged stresses (following Eqs. (16), (17) and (18)) are used in combination with scalar wind speed, the resulting values do not coincide with the preceding uniform behaviour. However, their enhancement is anticipated since scalar averaging results in higher values than vector averaging.

The combination of the averaging procedures with the shape of the profile used requires further investigation. It is a fact, though, that the scalar stresses overlap the traditional calculations at the high wind speed regime, where the theory is well known. In this range all methods converge, and the estimation of z_0 is safely and reasonably performed here. This procedure leads to values of 0.1, 0.3 and 1.0 m, for PIK, NOA and MAR, respectively.

Since all sites are located in complex terrain, topographical effects need to be taken into account in the calculations of z_0 . The NOA site is located on the top of a distinct hill; therefore, an underestimation of the roughness length is expected. The MAR site, on the other hand, lies on a gentle slope and topography is not expected to have any effects. Finally, although the PIK site is on a small hilltop it is surrounded by higher terrain, thus the final modifications to the wind profile are not obvious. In order to study possible important topographical influences, the MSFD micro-scaling wind flow simulation model (Walmsley *et al.* 1993) was used. The wind flow over the whole Attiki terrain was simulated and wind speed profiles were produced for every experimental site. The profiles were normalized in respect of an upwind profile, so as to determine the effects of terrain elevation on the flow. A distinct speedup of 12% in magnitude was observed in the case of NOA, while at both the MAR and the PIK sites terrain influences proved to be almost negligible. In this aspect, the above calculated z_0 values for MAR and PIK are considered valid, whereas a correction needs to be made for NOA. In order to quantify this underestimation of roughness, the drag-coefficient value at the respective height and wind speed interval was produced by MSFD for various model-input roughnesses. Coincidence with the previously presented experimental C_{Dn} value occurred for a roughness length of 0.6 m. In consequence, the z_0 used at NOA in this study has been increased to a value of 0.6 m compared to the initial estimate of 0.3 m.

4. RESULTS AND DISCUSSION

In the following figures the dependence of the dimensionless minimum friction velocity on the dimensionless roughness length z_0/h is presented for the three sites MAR, NOA and PIK, as well as for the historical data from the BOREX-95 experimental campaign. The calculation of U_*/W_* is performed by the methodologies described in section 2, that is by extracting the influence of the vector wind from the scalar averaged stresses. The preceding data analysis has provided estimates of the parameters involved, that is z_0 , h and the t -scale, for each particular data point. Among all historical data, namely TOGA COARE, SCOPE, BOREX-95 and LES, only the LES refer to what is supposed to be the minimum friction velocity, since they correspond to zero mean wind and scalar averaging. Therefore, LESs are also presented for reasons of comparison,

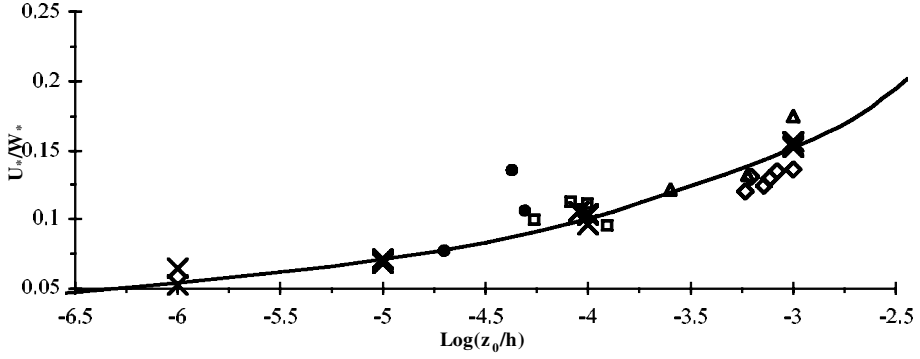


Figure 3. Dimensionless minimum friction velocity, $\tilde{U}_{*(c)}/W_*$, versus dimensionless roughness length, z_0/h , calculated for BOREX-95 (●), and data from MAR (◇), NOA (△) and PIK (□), using Eq. (20) to extract the vector wind contribution. Large-eddy simulation data (×) and Eq. (6) for $\beta = 0.8$ (—) are also presented. See Fig. 1 for locations and text for details.

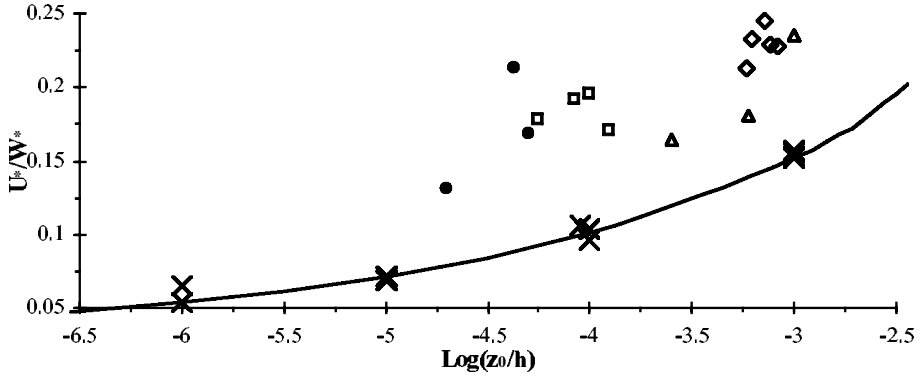


Figure 4. As Fig. 3 but using Eq. (21) to extract the vector wind contribution.

along with the theoretical model of Eq. (6). The fitting of Eq. (6) to LES is achieved for $\beta = 0.8$, by using the stability correcting function, Ψ_u , previously described (Grachev *et al.* 2000).

The dimensionless friction velocities, $\tilde{U}_{*(a)}/W_*$, as given by Eq. (20), for all data cases selected in this study, versus the respective dimensionless roughness lengths, z_0/h , are presented in Fig. 3. The results of using Eq. (21) for the minimum friction velocity calculation, noted as $\tilde{U}_{*(b)}$, are shown in Fig. 4. Finally, Fig. 5 illustrates the outcome of the third approach described in section 2(c). This is the dimensionless minimum friction velocity, hereafter $\tilde{U}_{*(c)}/W_*$, which is calculated by applying Eq. (10) to the result of Eq. (18), $\tilde{u}_{*(c)}$. The form of the stability correction function, Ψ_u , used in Eq. (10), is the one described in section 3(d) (Grachev *et al.* 2000). The relevant results from this method for $\tilde{u}_{*(a)}$ and $\tilde{u}_{*(b)}$ are not presented here since, as already discussed, both lead to higher values for the dimensionless minimum friction velocity compared to $\tilde{u}_{*(c)}$.

It is apparent, as a first conclusion from Figs. 3–5, that $\tilde{U}_{*(a)}$ as well as $\tilde{U}_{*(c)}$ give results that lie close to the LESs estimation for the minimum friction velocity. On the other hand, $\tilde{U}_{*(b)}$ results in remarkably larger values.

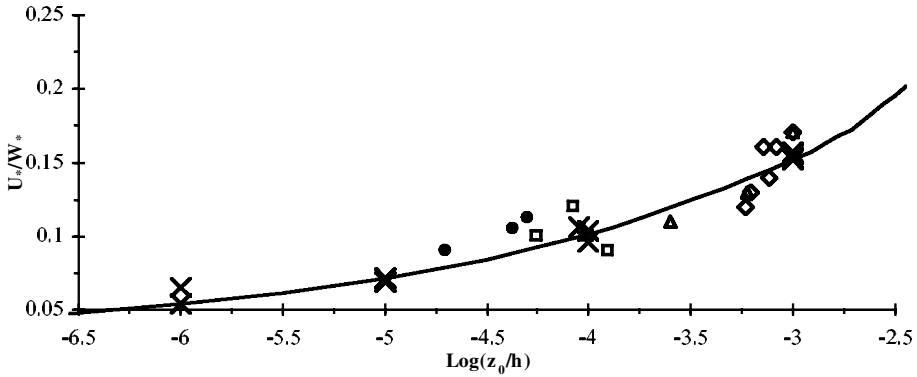


Figure 5. As Fig. 3 but using Eq. (10) to extract the vector wind contribution from the scalar-averaged stress of Eq. (18).

It is apparent that the first method for extraction giving $\tilde{U}_{*(a)}$, is the one closest to the methodology followed in the LES data by Schmidt and Schuman (1989). $\tilde{U}_{*(a)}$ is the standard deviation of the friction velocity (Eq. (20)), which coincides with the r.m.s. in the special case of a zero vector friction velocity. This holds true in shear-free convection, which is what LES simulated. Figure 3 shows an almost perfect coincidence between experimental and simulated results. The only exception is observed in one case of the BOREX-95 dataset. This could possibly be attributed to an inappropriate choice of the local time-scale t (section 3(b)) due to the unavailability of the full dataset. If a more accurate and representative scale could be considered, this result would probably collapse to the LES data. Such a possibility should be investigated. In conclusion, the overall apparent similarity is an indication that this particular methodology for extracting the mean wind shear proves efficient in relating real field data with the LES. Nevertheless, the latter is still a simulation of a natural process, although considered to be a reference study.

The second approach, $\tilde{U}_{*(b)}$ (Fig. 4), results in higher values compared to the other two methods as well as to the LES. The deviation of these values is also respectively large. This was expected since, as previously stated, this method is mathematically related to the fourth power. Taking this into account, the comparison with the LES may not have an apparent physical meaning. Thus, it would be ideal to recalculate LES using this particular formulation, that is the r.m.s. of the stresses instead of the friction velocities. In that case and despite the relative dispersion of these data, a better agreement with the LES would presumably be revealed.

Finally, the third approach using $\tilde{u}_{*(c)}$ also shows very good agreements with the LES reference data (Fig. 5). The procedure of extracting the wind shear is completely different in this methodology than in Eqs. (20) and (21). As commented in section 2(c), it implements the use of a theoretical wind profile combined with an averaging technique for the friction velocity given in Eq. (18). This particular averaging, $\tilde{u}_{*(c)}$, resembles the Sykes *et al.* (1993) methodology in their LES calculation. The results in Fig. 5 show that the application of Eq. (18) on experimental data combined with an extraction-by-profile methodology is quite promising, since field data almost coincide with the LESs. The results in Fig. 5 have been produced using the scalar wind given by Eq. (11). If the scalar wind corresponding to $\tilde{u}_{*(c)}$ was used (Eq. (19)) $\tilde{U}_{*(c)}/W_*$ would result in lower values. This would be due to the fact that Eq. (19) apparently gives a lower scalar wind

than Eq. (11), thus coefficient C would in that case be higher. Finally, an uncertainty of this approach is the definition of Ψ_u , which is open to discussion.

Another factor that could possibly affect the results, regardless of the averaging method followed, is the random sampling error, which is particularly severe for stress measurements under convective conditions. Despite the fact that significant effort has been made to reduce this error through appropriate selection of the cases studied, its elimination is not 100% feasible. It is apparent from Eqs. (16), (17) and (18) that the effect of the sampling error becomes larger in those averaging procedures incorporating larger exponents in the calculation. Thus, the results for U_{*c} (use of Eq. (18) in Eq. (10)) are the least affected, in contrast to U_{*b} , which is the minimum friction velocity most affected by the sampling error.

As an overall conclusion, it has to be noted that the investigation of the formulations proposed in this study is not intended to explicitly define a methodology for calculating the minimum friction velocity. The simplified concept of ‘right or wrong’ does not apply here. The objective definition of what is or what should be the minimum friction velocity, and consequently how it can be derived from experimental data, is still under question. These considerations lie beyond measuring problems or technical difficulties existing during light winds. What have been undertaken and presented in this study are three potential methods for calculating the minimum friction velocity, and their comparison with what the shear-free LES considered as such.

Recalling that the requirement for an accurate definition of the minimum friction velocity arises from the need for a correct calculation of the surface fluxes under convection, an alternative compromise that should be considered is a macroscopic approach instead of the microscopic one presented here. In particular, friction velocities could be measured indirectly through the influence they have on various processes, such as evaporation or deposition. For instance, an approach conceptually identical to Chamberlain’s (1966) original formulation for the analogous problem of evaporation or absorption could adopt the most suitable microscopic scheme in respect of the proper calculation of surface fluxes through their transport effects on scalar quantities.

5. CONCLUSIONS

In this study the influence of the mean vector wind speed on the value of the scalar wind, during strong convective regimes, was quantified through a new parameter C , which can be directly calculated from the experimental data. This parameter was also invoked in one of the three ways to calculate the dimensionless minimum friction velocity.

The methods for calculating the minimum friction velocity, examined in this work, consider scalar averaging procedures in order to avoid the obvious weakness of vector averaging in cases of shear-free convection. In particular, three different approaches have been considered and applied to three new experimental datasets, as no generally accepted formulation for the scalar stresses exists. The experimental values for the scalar average of the t -scaled friction velocities are in perfect agreement with the LES data. This behaviour was anticipated since this particular method resembles closely the methodology followed in the LES simulation. On the other hand, when the standard deviation of the stresses are processed their values were much higher and dispersed, in comparison to the LES data. This behaviour is consistent with the fact that the mathematical formulas representing the two methods are different. Recalculating the LESs using the second scheme would allow an objective comparison. The third approach accomplishes the extraction through a theoretical wind profile, a procedure that has been

physically justified. The values calculated according to this procedure were close to the LES data, although the concepts of these two methods are totally different.

The results for minimum friction velocity are presented in relation to the dimensionless roughness length, z_0/h . The values of $\log(z_0/h)$ for the three new sites analysed in this study range between -4.5 and -3 , which is nearly one order of magnitude larger than the previous historical datasets.

In conclusion, it should be noted that what has been undertaken and presented in this study comprises three potential methods for calculating the minimum friction velocity, and their respective comparison with what the shear-free LES considered as such. Nevertheless, a precise definition of the minimum friction velocity is under investigation, if the LESs are considered a simulation of nature. In order to justify these methods further, and clarify the meaning of the minimum friction velocity, further experimental work should be undertaken in respect of the effects that shear-free convection has on various other scalar quantities.

ACKNOWLEDGEMENTS

This work was supported by the EU Project SFINCS (Surface Fluxes IN Climate Systems), EC Contract ENV4-CT97-0573, and the Special Account for Research Grants of the University of Athens, Greece. The authors thank E. Batchvarova and S. E. Gryning for providing experimental data from MAR and NOA, A. A. Grachev for the data from BOREX-95, and the Hellenic National Meteorological Service for the radiosonde data of the Elliniko airport of Athens. Finally, the authors express their special thanks to S. S. Zilitinkevich for useful discussions.

REFERENCES

- | | | |
|---|------|---|
| Akylas, E., Tombrou, M.,
Lalas, D. P. and
Zilitinkevich, S. S. | 2001 | Surface fluxes under shear-free convection. <i>Q. J. R. Meteorol. Soc.</i> , 127 , 1–15 |
| Batchvarova, E. and Gryning, S. E. | 1998 | Meteorological measurements, wind climatology, atmospheric turbulence and internal boundary layer development in Athens during the Medcaphot-Trace Experiment. <i>Atmos. Environ.</i> , 32 , 2055–2069 |
| Beljaars, A. C. M. | 1995 | The parametrization of surface fluxes in large-scale models under free convection. <i>Q. J. R. Meteorol. Soc.</i> , 121 , 255–270 |
| Businger, J. A. | 1973 | A note on free convection. <i>Boundary-Layer Meteorol.</i> , 4 , 323–326 |
| Businger, J. A., Wyngaard, J. C. and
Izumi, Y. | 1971 | Flux profile relationships in the atmospheric surface layer. <i>J. Atmos. Sci.</i> , 28 , 181–189 |
| Chamberlain, A. C. | 1966 | Transport of gases to and from grass and grass-like surfaces. <i>Proc. R. Soc. London</i> , A290 , 236–265 |
| Deardorff, J. W. | 1970 | Convective velocity and temperature scales for the unstable planetary boundary layer. <i>J. Atmos. Sci.</i> , 27 , 1211–1213 |
| | 1972 | Parameterisation of the planetary boundary layer for use in general circulation models. <i>Mon. Weather Rev.</i> , 100 , 93–106 |
| Fairall, C. W., Bradley, E. F.,
Roger, D. P., Edson, J. B. and
Young, G. S. | 1996 | Air–sea flux parameterization in TOGA COARE. <i>J. Geophys. Res.</i> , 101 (C2), 3747–3764 |
| Grachev, A. A., Fairall, C. W. and
Larsen, S. E. | 1998 | On the determination of the neutral drag coefficient in the convective boundary layer. <i>Boundary-Layer Meteorol.</i> , 86 , 257–278 |
| Grachev, A. A., Fairall, C. W. and
Bradley, E. F. | 2000 | Convective profile constants revisited. <i>Boundary-Layer Meteorol.</i> , 94 , 495–515 |
| Højstrup, J. | 1982 | Velocity spectra in an unstable planetary boundary layer. <i>J. Atmos. Sci.</i> , 39 , 2239–2248 |
| Kropfli, R. A. and Clifford, S. F. | 1994 | The San Clemente Ocean Probing Experiment: A study of air–sea interactions with remote and <i>in-situ</i> sensors. IGARSS '94, Pasadena, CA. <i>IEEE</i> , 4 , 2407–2409 |
| Larsen, S. E. and
Zilitinkevich, S. S. (Eds.) | 2001 | ‘Surface fluxes in climate systems (SFINCS)’. Final report, Risø National Laboratory, Roskilde, Denmark |

- Mahrt, L., Vickers, D., Howell, J., Højstrup, J., Wilczak, J. M., Edson, J. and Hare, J. 1996 Sea surface drag coefficients in the Risø Air–Sea Experiment. *J. Geophys. Res.*, **101**(C6), 14327–14335
- Mikkelsen, T., Jørgensen, H. E., Lofstrom, P. and Lyck, E. 1996 ‘Borex-95: Experiment on concentration fluctuations: Data report RISØ-R-927(EN)’. RISØ National Laboratory, Department of Wind Energy and Atmospheric Physics, Roskilde, Denmark
- Paulson, C. A. 1970 The mathematical representation of wind speed and temperature profiles in the unstable atmospheric surface layer. *J. Appl. Meteorol.*, **9**, 857–861
- Schmidt, H. and Schumann, U. 1989 Coherent structure of the convective boundary layer derived from large-eddy simulations. *J. Fluid Mech.*, **200**, 511–562
- Schumann, U. 1988 Minimum friction velocity and heat transfer in the rough surface layer of a convective boundary layer. *Boundary-Layer Meteorol.*, **44**, 311–326
- Stull, R. B. 1988 *An introduction to boundary layer meteorology*. Kluwer Academic Publishers, Dordrecht, the Netherlands
- Sykes, R. I., Henn, D. S. and Lewellen, W. S. 1993 Surface-layer description under free-convection conditions. *Q. J. R. Meteorol. Soc.*, **119**, 409–421
- Walmsley, J. L., Weng, W., Karpic, S. R., Xu, D. and Taylor, P. A. 1994 Application of the Mixed Spectral Finite Difference (MSFD) model and its nonlinear extension (NLMSFD) to wind flow over Blashval hill. Pp. 263–271 in *Air pollution modelling and its application*. Eds. S. E. Gryning and M. M. Millan. Plenum Press, New York, USA
- Zilitinkevich, S. S., Grachev, A. A. and Hunt, J. C. R. 1998 Surface frictional processes and non-local heat/mass transfer in the shear-free convective boundary layer. Pp. 83–113 in *Buoyant convection in geophysical flows*. Eds. E. J. Plate, E. E. Fedorovich, D. X. Viegas and J. C. Wyngaard. Kluwer Academic Publishers, Dordrecht, the Netherlands